

# Effect of Confinement on the Properties of Sequestered Mixed Polar Solvents: Enzymatic Catalysis in Nonaqueous 1,4-Bis-2-ethylhexylsulfosuccinate Reverse Micelles

Andres M. Durantini,<sup>[b]</sup> R. Dario Falcone,<sup>[a]</sup> Juana J. Silber,<sup>[a]</sup> and N. Mariano Correa<sup>\*[a]</sup>

The influence of different glycerol, N,N-dimethylformamide (DMF) and water mixtures encapsulated in 1,4-bis-2-ethylhexylsulfosuccinate (AOT)/*n*-heptane reverse micelles (RMs) on the enzymatic hydrolysis of 2-naphthyl acetate by  $\alpha$ -chymotrypsin is demonstrated. In the case of the mixtures with DMF and protic solvents it has been previously shown, using absorption, emission and dynamic light-scattering techniques, that solvents are segregated inside the polar core of the RMs. Protic solvents anchor to the AOT, whereas DMF locates to the polar

core of the aggregate. Thus, DMF not only helps to solubilize the hydrophobic substrate, increasing its effective concentrations but surprisingly, it does not affect the enzyme activity. The importance of ensuring the presence of RMs, encapsulation of the polar solvents and the corrections by substrate partitioning in order to obtain reliable conclusions is highlighted. Moreover, the effect of a constrained environment on solvent-solvent interactions in homogenous media and its impact on the use of RMs as nanoreactors is stressed.

## 1. Introduction

The majority of the chemical reactions that occur in biology take place at the interface of cell organelles rather than in a medium outside the cell. It is therefore important to understand the interactions of proteins with those interfaces. Even if reverse micelles (RMs) are an oversimplified model, the amphipathic essence of biological membranes is preserved and important properties such as hydrogen bonding tendencies can be studied.<sup>[1]</sup> RMs are formed by surfactant molecules dissolved in nonpolar solvents with their polar head groups pointing inward and the hydrocarbon chains pointing out to the solvent.<sup>[2–4]</sup> Sodium 1,4-bis-2-ethylhexylsulfocuccinate (AOT) is one of the most investigated and used anionic surfactants because it forms stable RMs without the addition of co-surfactants.<sup>[2–5]</sup> AOT RMs can encapsulate different amounts of water, expressed as  $W_0$  ( $W_0 = [\text{water}]/[\text{AOT}]$ ), depending on the nonpolar solvent used, addition of solutes, and temperature.<sup>[4,6,7]</sup> The most common solvent used to be dispersed is water but polar organic solvents, which have high dielectric constants and low solubility in the nonpolar solvent, can also be sequestered by the surfactant forming the nonaqueous RMs.<sup>[8]</sup> Some of these polar solvents include dimethylsulfoxide (DMSO), formamide, *N,N*-dimethylformamide (DMF), *N,N*-dimethylaceta-

mid, ethylene glycol, propylene glycol, glycerol (GY) and ethyl lactate.<sup>[8–10]</sup> Also, mixtures of polar solvents can remain encapsulated within the RM polar core; if that happens, their pure or “bulk” solvent structure changes dramatically and segregation of the solvents occurs. Nonaqueous RMs and those in polar solvent mixtures have been shown to be useful as nanoreactors.<sup>[8]</sup> Studies have shown that protic solvents anchor to the polar side of the AOT/*n*-heptane RMs interface, whereas aprotic solvents form the polar core that interacts with the sodium counterions.<sup>[9–11]</sup> Specifically, in reference [11] we showed for the first time segregation of GY molecules at the polar side of the AOT RMs interface, whereas the DMF molecules remained in the polar core. Those findings motivated us to investigate if such solvent segregation might favor the outcome of chemical reactions.

Studies performed in our group indicated that the size of RMs not only depends on the quantity of polar solvent added, but also on the interaction of the polar solvent with the RMs interface.<sup>[10,12]</sup> This is an interesting feature of the RMs in the context of nanoreactors, because not only the size but also the polar solvent structure can be controlled upon encapsulation.

Since the pioneering works of Martinek et al.<sup>[13]</sup> were published more than 30 years ago, it has become known that, by using water as the dispersed solvent, the catalytic activity of different enzymes can be enhanced by the juxtaposed solvent effects.<sup>[2,13–23]</sup> In particular, these effects have been well established for  $\alpha$ -chymotrypsin ( $\alpha$ -CT), which, being a hydrophilic and globular enzyme, usually remains incorporated within the RMs.<sup>[14,20]</sup> Interestingly, the group of A. J. Wand has developed a method to examine the structure of certain proteins in different RMs with water as a polar solvent by using high-resolution NMR spectroscopy.<sup>[24,25]</sup> In their efforts to encapsulate proteins with high structural fidelity in AOT RMs under these particular

[a] Dr. R. D. Falcone, Dr. J. J. Silber, Dr. N. M. Correa  
Departamento de Química, Universidad Nacional de Río Cuarto  
Agencia Postal # 3. C.P. X5804BYA Río Cuarto (Argentina)  
E-mail: mcorrea@exa.unrc.edu.ar

[b] Dr. A. M. Durantini  
Department of Chemistry and Center  
for Self-Assembled Chemical Structures  
McGill University, 801 Sherbrooke Street West  
Montreal, Quebec H3A 0B8 (Canada)

Supporting Information and the ORCID identification number(s) for the author(s) of this article can be found under <http://dx.doi.org/10.1002/cphc.201501190>.

experimental conditions, they showed that this surfactant has a strong denaturing effect on most of the proteins investigated that were located in the water pool; however  $\alpha$ -CT has not been studied in these experiments. This represents an avenue of investigation, as it seems that enzymes can function upon confinement, even though NMR data shows changes in their conformation. Conversely, there are no reports of NMR studies on nonaqueous AOT RMs and enzymes that are located at the polar side of the RMs interface and not in the polar core.

By contrast, the substrates for  $\alpha$ -CT in a living organism are normally esters or peptides with low water solubility and the hydrolysis reaction take place within a hydrophobic domain. In order to mimic the physiological situation, *in vitro*, it is important to design a nanoreactor that can bring the hydrophobic substrate to the reaction milieu, in which the enzyme is located. Also, it should bring about an improvement in the enzyme activity. For organic nonpolar substrates in homogeneous media, the use solvents in which they have increased solubility, such as DMF or DMSO, will be required. One problem is that DMSO acts as denaturant for  $\alpha$ -CT,<sup>[26]</sup> and in DMF the enzyme has been shown to be severely inactivated at low water content.<sup>[27,28]</sup> A question therefore arises: it possible to create such nanoreactors using RMs, water, and solvents such as DMF and DMSO? Because of the unique properties of the AOT RMs mentioned above, the answer is yes, and this article shows how to create such an enzymatic reactor and also how to handle the data in order to obtain the "true" enzymatic parameters that take into account the substrate partition between the RMs and the external solvent pseudophase.<sup>[14,20]</sup> Surprisingly, there are no reports in the literature that demonstrate enzymatic reactions using binary polar solvent mixtures for confinement in RMs.

The first studies performed on the catalytic behavior of  $\alpha$ -CT in RM-containing media have been done using water as the polar solvent encapsulated in the core of the aggregates.<sup>[14]</sup> However, in the last 10 years the properties of the enzyme have also been studied in other solvents, such as GY and DMSO, as well as their binary mixtures with water.<sup>[8,20,26]</sup> Falcone et al.<sup>[20]</sup> investigated the kinetics of the enzymatic hydrolysis of 2-naphthyl acetate (2-NA) by  $\alpha$ -CT in AOT RMs designed with GY and GY/water (38% *v/v*) mixtures /AOT/*n*-heptane. It was demonstrated that addition of GY to the RMs results in enhanced catalytic efficiency of  $\alpha$ -CT. GY addition decreases the conformational mobility of  $\alpha$ -CT, thus increasing enzyme stability and activity.<sup>[20]</sup>

Recently, Moyano et al.<sup>[26]</sup> have studied the kinetics of the enzymatic hydrolysis of *N*-benzoyl-L-tyrosine *p*-nitroanilide by  $\alpha$ -CT in homogenous media and in DMSO/water/AOT/*n*-heptane RMs, at different DMSO/water content. In homogeneous media, as expected, DMSO acts as a denaturant of the protein and a dramatic decrease in the enzymatic activity was found at higher DMSO contents. However, upon DMSO/water mixture confinement, the hydrogen-bond interactions between DMSO and water are disrupted; water remains at the polar side of the AOT RMs interface where the enzyme is located, and DMSO molecules migrate to the polar micelle core and help solubilize the substrate. The overall result is an increase in the effective

concentration inside the RM and the consequent enhancement in the reaction rate. For the first time, we show that the use of a denaturant solvent in a confined environment increases the enzyme activity.

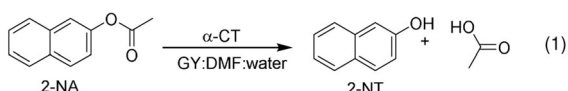
Our goal, motivated by our pioneering studies on of solvent segregation inside AOT RMs,<sup>[11]</sup> was to ascertain if other nanoreactors can be designed such that an enzymatic deactivating solvent in homogeneous solution is used in a confined environment. We sought to determine if there is an improvement in the substrate solubility within the RMs without affecting enzyme performance. To this end, two binary (GY/water and DMF/water) and one ternary (GY/DMF/water) solvent mixtures were investigated for the  $\alpha$ -CT-catalyzed hydrolysis of 2-NA in homogenous and AOT/*n*-heptane RMs systems. These are interesting systems because GY is a polyol that stabilizes biological molecules such as proteins and enzymes in water.<sup>[29–32]</sup> DMF, in which 2-NA is very soluble, is of particular interest due to the lack of a hydrogen atom that is capable of engaging in hydrogen-bond interactions and because its bulk structure is altered in aqueous mixtures.<sup>[33]</sup> Although DMF is one of the most important aprotic organic solvents used in a wide variety of chemical applications, its use severely decreases the enzyme activity in homogeneous solution.<sup>[28]</sup> The use of the ternary mixture is justified by our previous results that showed a favorable effect if GY was added to the aqueous pool of the RMs.<sup>[20]</sup> We therefore expected that the presence of GY would improve the catalytic activity of  $\alpha$ -CT in the presence of DMF. It should be considered that water is always necessary for the hydrolysis reaction to occur. The proposed mechanism of the reaction and the kinetic equations are detailed in the Supporting Information.

In summary, we show that everything that happens in homogeneous solution has to be reconsidered because of the fascinating effect of confinement.

## 2. Results and Discussion

In this work, we studied reactions in the following mixtures: GY/water (40:60, *v/v*), DMF/water (20:80, *v/v*) and GY/DMF/water (20:20:60, *v/v/v*), in homogeneous media (this refers to the solvent mixture not encapsulated inside the RMs) and encapsulated in AOT/*n*-heptane RMs. In a confined environment, results were obtained at  $W_T$  values [ $W_T = ([GY] + [DMF] + [water])/[AOT] = W_{GY} + W_{DMF} + W_{water}$ ] of around 4 to 6 because this represents the best set of conditions found for the enzymatic reaction. At lower  $W_T$  values the reaction is very slow, and at higher  $W_T$  the RMs become unstable in the ternary mixture.

The reactions were followed spectrophotometrically by the increase at the maximum of the product 2-naphthol (2-NT) absorption band ( $\lambda_{max} = 327$  nm) at  $25.0 \pm 0.5$  °C. Absorbance was recorded on a Hewlett-Packard 8453 UV/Vis spectrophotometer equipped with a thermostated cell (volume 3 mL, path length 1 cm). The UV/Vis spectroscopic analysis shows that the  $\alpha$ -CT-catalyzed hydrolysis of 2-NA in all the mixtures and in water, produced 2-NT in quantitative yield [Eq. (1)]:



As the DMF/water and GY/DMF/water mixtures were never previously studied inside AOT RMs, the following question needs answering: Is this surfactant actually forming RMs with those polar solvents? That is, before proceeding with the kinetic studies it is necessary to evaluate if the mixtures are effectively sequestered by AOT in order to form RMs. As has been discussed in the literature,<sup>[8]</sup> GY, DMF and water and their mixtures have very low solubility in *n*-heptane. Thus, the various mixtures of polar solvents cannot be dissolved in this organic pseudophase. It is often reported in the literature that because a transparent solution is obtained when polar solvents are mixed with the surfactant, RMs are created. This is absolutely incorrect because an RM medium needs to organize its components into the interface and the polar core.<sup>[8]</sup> Thus, when a new system is investigated it is mandatory to effectively demonstrate that the polar solvents are encapsulated by the surfactants creating organized systems with their unique properties. Furthermore,  $\alpha$ -CT has a diameter of about 4 nm,<sup>[34,35]</sup> which generates doubt about whether the encapsulation of  $\alpha$ -CT affect the diameter of the differently organized systems.

As shown in several studies, dynamic light scattering (DLS) is a good technique for investigating these types of assemblies and, it accurately reveals whether the solvents are encapsulated by the surfactants. Moreover, this technique can also estimate the shape of the droplets and if they interact with each other. In all the systems investigated, the droplet size value increases with a linearly with  $W_T$  (results not shown), indicating that the different polar solvent mixtures are effectively encapsulated in the RMs.<sup>[4,6–10,36,37]</sup>

The diameters and polydispersities of the RMs are listed in Table 1 at a given value,  $W_T=6$ . Table 1 shows that the diameter increases with the presence of GY and remains almost constant as DMF content is varied. Also, the sizes of GY/water and GY/DMF/water/AOT/*n*-heptane RMs are very similar. According to these results, when the binary or ternary mixtures are dissolved, GY and water are bound by hydrogen-bond interactions with the AOT polar head group at the interface of the

Media	$d_{app}$ [nm]	Polydispersity [%]
water/AOT/ <i>n</i> -heptane	5.6	7
water/AOT/ <i>n</i> -heptane + $\alpha$ -CT	5.7	8
GY/water (40:60, v/v)/AOT/ <i>n</i> -heptane	20.1	3
GY/water (40:60, v/v)/AOT/ <i>n</i> -heptane + $\alpha$ -CT	20.1	5
DMF/water (20:80, v/v)/AOT/ <i>n</i> -heptane	6.5	2
DMF/water (20:80, v/v)/AOT/ <i>n</i> -heptane + $\alpha$ -CT	6.8	2
GY/DMF/water (20:20:60, v/v/v)/AOT/ <i>n</i> -heptane	18.9	8
GY/DMF/water (20:20:60, v/v/v)/AOT/ <i>n</i> -heptane + $\alpha$ -CT	18.2	7

[a]  $W_0=6$ ,  $W_T=6$ ; [ $\alpha$ -CT] =  $5 \times 10^{-6}$  M;  $T=25^\circ\text{C}$ .

RMs and DMF molecules remain in the RM core, engaging in electrostatic interactions with sodium counterions as was previously found for the individual solvents.<sup>[12]</sup>

The results summarized in Table 1 also demonstrate that the presence of the enzyme does not affect the size of the different RMs systems, because the droplets are essentially the same size with and without the enzyme.

$\alpha$ -CT was analyzed by using fluorescence emission spectroscopy, by monitoring the emission band of the tryptophan residue centered at  $\lambda_{em}=350$  nm. The spectrum of the enzyme dissolved in solution containing 8 M urea showed that its conformational structure was altered because of the denaturing effect of the solute. In this sense if any of the polar solvents used here are denaturing agents for the enzyme, the emission band should appear around  $\lambda_{em} \approx 350$  nm. The results obtained with the polar solvent blends are shown in Figure 1 at  $\lambda_{exc} \approx 280$  nm. As is apparent, the emission profile for  $\alpha$ -CT is not altered in any mixture studied in homogeneous and AOT RMs.

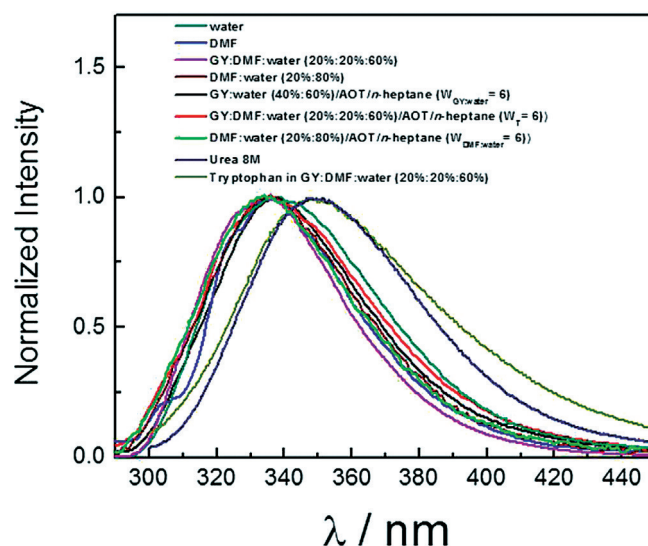


**Figure 1.** Normalized emission spectra of  $\alpha$ -CT in different media.  $\lambda_{exc}=280$  nm; [ $\alpha$ -CT] =  $5 \times 10^{-6}$  M, [AOT] = 0.1 M.

It seems that encapsulation of the enzyme in the AOT RM media does not significantly alter the tertiary structure of  $\alpha$ -CT.

Next, we discuss the hydrolysis reaction in homogenous solution in which DMF and GY were used as a part of the polar component in order to improve the 2-NA solubility in water. Does DMF have any effect on the enzymatic hydrolysis? We have shown (Figure 1) that it does not affect the enzyme tertiary structure, but what about the  $\alpha$ -CT activity?

The hydrolysis rates of the enzymatic reaction were followed by absorption spectroscopy at the product absorption band in every media. The best mechanism to explain the experimental data is the classical Michaelis–Menten mechanism. The kinetic parameters were determined by fitting the experimental data as described in the Supporting Information. Accordingly, the catalytic rate constant ( $k_{cat}$ ), the Michaelis–Menten constant ( $K_M$ ) and the catalytic efficiency ( $k_{cat}/K_M$ ) were calculated.

## 2.1. Reaction in Homogeneous Media: DMF/Water and GY/DMF/Water Mixtures

Typical absorption spectra for hydrolysis of 2-NA at different reaction times in GY/DMF/water (20:20:60, v/v/v) are shown in Figure S2 (in the Supporting Information), and the formation of the product 2-NT is evident [Eq. (1)]. Similar results were obtained in DMF/water (results not shown).

A plot of  $v_0/[\alpha\text{-CT}]$  versus the analytical concentration of 2-NA ( $[2\text{-NA}]_T$ ) is shown in Figure S3A. Figure S3B shows a typical result obtained by treating the data as a Lineweaver–Burk plot [Eq. (S6)], the linearity of which indicates that, under the conditions used, the Michaelis–Menten mechanism applies in the polar solvent mixtures as has been previously found for water and GY/water mixtures.<sup>[20,38]</sup> Although kinetic constants could be obtained from the linear fit using the Equation S6, throughout this work we determined the kinetic parameters  $k_{\text{cat}}$  and  $K_M$  using a nonlinear fit according to Equation S4. The results are shown in Table 2, which gives the values obtained for the rate constants in DMF/water (20:80, v/v) and GY/DMF/water (20:20:60, v/v/v) mixtures, where  $(k_{\text{cat}}^{\text{exp}})^{\text{mixture}}$  is the experimental catalytic constant and  $(K_M^{\text{exp}})^{\text{mixture}}$  is the experimental Michaelis–Menten constant. Also, the results from reference [20] obtained in water and in a GY/water (32:68, v/v) mixture are included for comparison. Table 2 shows that the catalytic efficiency of the enzyme, given by the ratio  $(k_{\text{cat}}^{\text{exp}}/K_M^{\text{exp}})^{\text{mixture}}$ , is much smaller for reactions occurring in binary or ternary DMF-containing mixtures in comparison with the GY/water mixture. A dramatic decrease in the catalytic efficiency value can be observed if only DMF and water is used, as previously shown for other enzymatic reactions.<sup>[27,28]</sup> The increase of the enzymatic catalytic efficiency found for the GY/water mixture compared with the DMF/water and GY/DMF/water mixtures is due to both an increase in  $(k_{\text{cat}}^{\text{exp}})^{\text{mixture}}$  and a reduction in  $(K_M^{\text{exp}})^{\text{mixture}}$  values. The results demonstrate that DMF has a negative effect on the enzyme activity, affecting dramatically its hydration level or conformational structure but without denaturing the enzyme (Figure 1).<sup>[28]</sup>

In contrast, it was observed that the 2-NA solubility increases markedly if DMF is present in the binary and ternary mixtures. Table 3 shows the  $K_p$  values for 2-NA in the different mixtures investigated. Absorption spectroscopy was used to obtain these data and details are provided in the Supporting

Medium	$(k_{\text{cat}}^{\text{exp}})^{\text{mixture}}$ [ $\times 10^{-2} \text{ s}^{-1}$ ]	$(K_M^{\text{exp}})^{\text{mixture}}$ [ $\times 10^{-3} \text{ M}$ ]	$(k_{\text{cat}}^{\text{exp}}/K_M^{\text{exp}})^{\text{mixture}}$ [ $\text{M}^{-1} \text{ s}^{-1}$ ]
water <sup>[b]</sup>	2.10 ± 0.21	0.57 ± 0.06	36.00
GY/water (38:62, v/v) <sup>[b]</sup>	8.80 ± 0.88	0.31 ± 0.03	284.00
GY/DMF/water (20:20:60, v/v/v)	0.37 ± 0.04	0.64 ± 0.04	5.78
DMF/water (20:80, v/v)	0.21 ± 0.04	3.32 ± 0.02	0.62

[a]  $[\alpha\text{-CT}] = 5 \times 10^{-6} \text{ M}$ . [b] Values obtained from reference [20].

**Table 3.**  $K_p$  and  $K_p^{\text{mixture}/n\text{-heptane}}$  values for the different RM systems and homogenous mixtures.<sup>[a]</sup>

Medium	$K_p$	$K_p^{\text{mixture}/n\text{-heptane}}$ ( $\times 10^{-2}$ )
<b>RMs</b>		
water/AOT/ <i>n</i> -heptane	0.92 ± 0.05	–
GY/water (38:62, v/v)/AOT/ <i>n</i> -heptane	5.65 ± 0.73	–
DMF/water (20:80, v/v)/AOT/ <i>n</i> -heptane	20.68 ± 2.30	–
GY/DMF/water (20:20:60, v/v/v)/AOT/ <i>n</i> -heptane	15.7 ± 0.79	–
<b>Homogeneous media</b>		
water <sup>[b]</sup>	–	0.36 ± 0.02
GY/water (38:62, v/v) <sup>[b]</sup>	–	0.66 ± 0.03
DMF/water (20:80, v/v)	–	4.03 ± 0.03
GY/DMF/water (20:20:60, v/v/v)	–	3.01 ± 0.15

[a]  $[2\text{-NA}] = 1 \times 10^{-3} \text{ M}$ ,  $[\alpha\text{-CT}] = 5 \times 10^{-6} \text{ M}$ . [b] Values obtained from reference [20].

Information. If DMF is present in the water mixture the  $K_p$  values increase considerably, that is, 2-NA is more soluble in the water mixture than in *n*-heptane. However, a striking decrease of the  $\alpha\text{-CT}$  efficiency was found when DMF was added, even though the solubility of the substrate increases markedly.

## 2.2. Reactions in AOT/*n*-Heptane RMs

The hydrolysis reaction was studied in the following RMs systems: water/AOT/*n*-heptane, GY/water (40:60, v/v)/AOT/*n*-heptane, DMF/water (20:80, v/v)/AOT/*n*-heptane, and GY/DMF/water (20:20:60, v/v/v)/AOT/*n*-heptane. It is important to recall that all the studies were performed at the maximum  $W_T$  value that can be achieved for GY/DMF/water (20:20:60, v/v/v)/AOT/*n*-heptane RMs, that is  $W_T = 6$ .

We have previously studied this reaction in water/AOT/*n*-heptane and GY/water (38:62% v/v)/AOT/*n*-heptane RMs, albeit at  $W_T = 13.2$ .<sup>[20]</sup> Therefore, in order to compare these results with the one obtained here, the kinetic parameters were investigated at  $W_0 = 6$  and  $W_T = 6$ . Knowing the location and properties of each of the polar solvents both alone and in the mixtures within AOT RMs, a systematic study of the hydrolysis reaction of the substrate 2-NA was made for each system.<sup>[8,9,20]</sup>

From the data in Figures S4A, S5A, S6A and S7A it is possible to observe how the initial rate increases upon increasing the substrate concentration at constant enzyme concentration ( $[\alpha\text{-CT}] = 5 \times 10^{-6} \text{ M}$ ) for all the systems studied. As in homogeneous media, if the substrate concentration is high,  $v_0$  is essentially independent of the substrate concentration. Figures S4B, S5B, S6B and S7B indicate that the reaction mechanism inside the RMs follows the Michaelis–Menten kinetics as straight lines are obtained in the Lineweaver–Burk plots.

Typical results obtained on the effect of varying the AOT concentration on the relationship between  $v_0/[\alpha\text{-CT}]$  and the analytical concentration of 2-NA at  $W_T = 6$  are shown in Figure 2 for GY/DMF/water (20:20:60, v/v/v)/AOT/*n*-heptane RMs. This data shows that the  $v_0/[\alpha\text{-CT}]$  ratio is lower at higher concentrations of AOT.

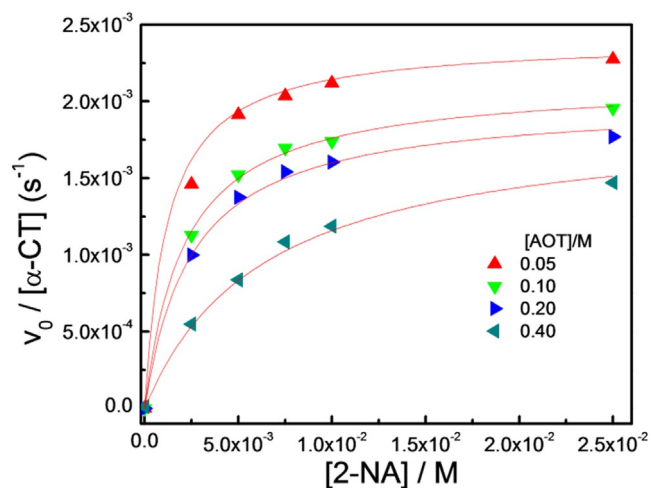


**Figure 2.** Effect of AOT concentration on the relationship between the initial rate of reaction (per enzyme) and the analytical concentration of 2-NA in reverse micelles of GY/DMF/water (20:20:60, v/v/v)/AOT/*n*-heptane at  $W_T = 6$ .  $[\alpha\text{-CT}] = 5 \times 10^{-6}$  M.

The dependence on the surfactant concentration can be attributed to three factors:<sup>[14,38]</sup> 1) changes in the size, shape and microscopic properties of the RMs; 2) changes in the properties of the enzyme; and 3) the substrate distribution between different RM pseudophases. As Table 1 shows that the droplet sizes are the same with or without  $\alpha$ -CT, factor 1 can be discarded. As discussed before,  $\alpha$ -CT remains totally associated to the RMs. Besides, the emission spectra do not show denaturation of the enzyme (Figure 1), a fact which allows us also to discard factor 2. In addition, as shown by the experimental kinetic parameters obtained at different [AOT] (Table 4), the values of the experimental catalytic constant within the RMs,  $(k_{\text{cat}}^{\text{exp}})^{\text{mic}}$ , are practically constant at all the surfactant concentrations used. The same results were obtained for other mixtures studied. It is known that by varying of the AOT concentration, but keeping  $W$  constant, the shape and the size of the RMs are maintained.<sup>[4,39]</sup> Thus, no variation in  $k_{\text{cat}}$  with [AOT] was expected. On the contrary, there is an increase in the experimental Michaelis–Menten constant in the RMs  $(K_M^{\text{exp}})^{\text{mic}}$  (Table 4 and Figure S8), which reflects the distribution of the substrate between the micelles and the external solvent. The differences in the kinetic profiles shown in Figure 2 can be attributed to partitioning of the substrate between the micellar pseudophase and the external solvent. This distribution has to be taken into

**Table 4.** Summary of experimental kinetic parameters of the enzymatic reaction in GY/DMF/water (20:20:60, v/v/v)/AOT/*n*-heptane RMs at different [AOT].<sup>[a]</sup>

[AOT] [M]	$(k_{\text{cat}}^{\text{exp}})^{\text{mic}}$ [ $\times 10^{-2} \text{ s}^{-1}$ ]	$(K_M^{\text{exp}})^{\text{mic}}$ [ $\times 10^{-2} \text{ M}$ ]	$(k_{\text{cat}}^{\text{exp}}/K_M^{\text{exp}})^{\text{mic}}$ [ $\text{M}^{-1} \text{ s}^{-1}$ ]
0.05	$0.22 \pm 0.02$	$0.11 \pm 0.02$	2.0
0.10	$0.20 \pm 0.01$	$0.20 \pm 0.01$	1.0
0.20	$0.21 \pm 0.01$	$0.30 \pm 0.02$	0.7
0.40	$0.19 \pm 0.01$	$0.64 \pm 0.03$	0.3

[a]  $W_T = 6$ ;  $[\alpha\text{-CT}] = 5 \times 10^{-6}$  M;  $T = 25^\circ\text{C}$ .

consideration in order to obtain the enzymatic kinetic parameters in the RM media. This correction factor is not always to be found among the vast literature on enzymatic catalysis. The values of  $(K_M^{\text{exp}})^{\text{mic}}$  were corrected by the partitioning of 2-NA ( $K_p$ ) with Equation (2).<sup>[14,20,40]</sup>  $K_p$  values were obtained using the procedure described in the Supporting Information and are gathered in Table 3.

$$(K_M^{\text{corr}})^{\text{mic}} = \frac{(K_M^{\text{exp}})^{\text{mic}}}{(1 + K_p[\text{AOT}])} \quad (2)$$

These results are listed in Table 5 from which it can be seen that the corrected catalytic efficiency values,  $(k_{\text{cat}}^{\text{exp}}/K_M^{\text{corr}})^{\text{mic}}$ , are larger than the efficiency obtained for those uncorrected,  $(k_{\text{cat}}^{\text{exp}}/K_M^{\text{exp}})^{\text{mic}}$ . Furthermore, the values of  $(k_{\text{cat}}^{\text{exp}}/K_M^{\text{corr}})^{\text{mic}}$  obtained for the encapsulated mixtures are larger than those obtained for the reaction that occurs in RMs encapsulating only water. Note that the largest  $(k_{\text{cat}}^{\text{exp}}/K_M^{\text{corr}})^{\text{mic}}$  values correspond to the mixture with DMF, which is interesting because the exact opposite result was found in homogenous media (Table 2).

**Table 5.** Summary of experimental kinetics parameters of the enzymatic reaction in different RMs systems.

RM	$(K_M^{\text{corr}})^{\text{mic}}$ [ $\times 10^{-2} \text{ M}$ ]	$(k_{\text{cat}}^{\text{exp}}/K_M^{\text{corr}})^{\text{mic}}$ [ $\text{M}^{-1} \text{ s}^{-1}$ ]	$(k_{\text{cat}}^{\text{exp}}/K_M^{\text{exp}})^{\text{mic}}$ [ $\text{M}^{-1} \text{ s}^{-1}$ ]
water/AOT/ <i>n</i> -heptane	$0.30 \pm 0.01$	0.9	0.6
GY/water (40:60, v/v)/AOT/ <i>n</i> -heptane	$0.70 \pm 0.02$	2.2	1.5
DMF/water (20:80, v/v)/AOT/ <i>n</i> -heptane	$0.29 \pm 0.02$	4.5	1.4
GY/DMF/water (20:20:60, v/v/v)/AOT/ <i>n</i> -heptane	$0.07 \pm 0.02$	2.9	1.0

Herein, the correction made by the substrate partition allows a comparison to be made of the kinetic parameters among different RMs media, independent of the external solvent and the polar solvent mixtures encapsulated in the polar core of the RMs. Nevertheless, it is not possible to compare the data with homogeneous media. To do that, it is necessary to know the substrate partition between the different solvent mixtures and the external solvent used (*n*-heptane) but in the absence of the surfactant. In other words, in order to make a significant comparison of the kinetic parameter values obtained for the AOT RMs with the values obtained in homogeneous medium it is necessary to express the values in terms of a common thermodynamic substrate activity scale and not in terms of substrate concentrations.<sup>[20,26,41]</sup> The simplest way to do that is to compare the rate constants, taking as the reference the external solvent of the RMs (*n*-heptane). The catalytic efficiency of the enzymatic reaction obtained in the bulk solvents,  $(k_{\text{cat}}^{\text{exp}}/K_M^{\text{exp}})^{\text{mixture}}$ , must be corrected by substrate partitioning between the polar mixtures and *n*-heptane  $(K_p^{\text{mixture}/n\text{-heptane}})$ , which were calculated (Supporting Information) and gathered in Table 3. This correction is expressed as Equation (3):

$$(K_M^{\text{corr}})^{\text{mixture}} = (K_M^{\text{exp}})^{\text{mixture}} / K_p^{\text{mixture}/n\text{-heptane}} \quad (3)$$

Table 3 list the  $k_p^{\text{mixture}/n\text{-heptane}}$  values obtained for the polar solvent mixtures and pure water in homogenous media. These values indicate the ability of the DMF to solubilize the substrate with the distribution constant much larger for the DMF/water and GY/DMF/water mixtures than for pure water and also larger compared to the GY/water mixture.

Table 6 summarizes the values of the corrected catalytic efficiencies ( $k_{\text{cat}}^{\text{exp}}/K_M^{\text{corr}}$ ) obtained using Equation (3). The  $k_{\text{cat}}^{\text{exp}}/K_M^{\text{corr}}$  values for the DMF/water (20:80, v/v)/AOT/*n*-heptane and GY/DMF/water (20:20:60, v/v/v)/AOT/*n*-heptane RMs are

Table 6. Summary of experimental kinetics parameters of the enzymatic reaction in the different homogeneous mixtures and RMs systems.		
Medium	$k_{\text{cat}}^{\text{exp}}/K_M$ [s <sup>-1</sup> M <sup>-1</sup> ]	$k_{\text{cat}}^{\text{exp}}/K_M^{\text{corr}}$ [s <sup>-1</sup> M <sup>-1</sup> ]
<b>Homogeneous media</b>		
water <sup>[a]</sup>	36.0	0.10
GY/water (38:62, v/v) <sup>[a]</sup>	284.0	1.80
DMF/water (20:80, v/v)	0.62	0.025
GY/DMF/water (20:20:60, v/v/v)	5.80	0.12
<b>RM</b>		
water/AOT/ <i>n</i> -heptane		0.90
GY/water (40:60, v/v)/AOT/ <i>n</i> -heptane		2.20
DMF/water (20:80, v/v)/AOT/ <i>n</i> -heptane		4.50
GY/DMF/water (20:20:60, v/v/v)/AOT/ <i>n</i> -heptane		2.90
[a] Values obtained from reference [20].		

larger than for the water/AOT/*n*-heptane RMs and are of the same order of magnitude as for the GY/water encapsulated mixture. A comparison of the RM media with homogenous media for the same mixtures shows that the  $k_{\text{cat}}^{\text{exp}}/K_M^{\text{corr}}$  value is 24 times larger if the ternary mixture is encapsulated and 180 times larger if the binary mixture is encapsulated (Table 6). The lowest  $k_{\text{cat}}^{\text{exp}}/K_M^{\text{corr}}$  value in homogenous media corresponds to the mixture with DMF, which is consistent with the dehydrating and conformational effect that this solvent has on the enzyme. However, and in contrast to what happens in homogenous medium, in the RM media the greatest catalytic efficiency is achieved for the encapsulated DMF-containing mixture.

These data can be explained by considering what we learn about the behavior of polar solvent mixtures upon encapsulation by using different techniques such as electronic spectroscopy and DLS.<sup>[9–12]</sup> Hence, for reactions occurring in different systems, the solvent within the micelle acquires a particular location such that the stability of the enzyme is always favored. GY increases the catalytic efficiency of the enzyme by reducing its conformational mobility. GY has also been found to readily form a polyol hydrogen-bond network that fixes the structure of the protein in a more rigid matrix.<sup>[20]</sup> Also, water is essential for the enzyme to perform its function as a hydrolase.<sup>[14]</sup> For this reason, for encapsulation of only the binary GY/DMF mixture, the reaction does not occur. Water and GY are placed at the polar side of the AOT RM interface and we hypothesize that the enzyme is located this place of the AOT RMs interface, surrounded by the solvents. Otherwise, and in concordance

with the results observed in homogenous media, if the enzyme was interacting with DMF molecules, its enzymatic activity would be dramatically reduced. We estimate that the polar core of the aggregate is where DMF interacts with the surfactant's sodium counterions. Thus, the reaction occurs at the RM–polar solvent interface rich in GY and water molecules and, a synergistic contribution to the activity and efficiency of  $\alpha$ -CT was observed for the reaction in confined media.

### 3. Conclusions

We have shown that although DMF is a polar solvent that inhibits the catalytic activity of  $\alpha$ -CT in homogeneous DMF/water and GY/DMF/water mixtures, upon encapsulation in AOT RMs, the situation changes. DMF is excluded from the interface at which the reaction occurs, but helps to solubilize the substrate, thus increasing the rate of the hydrolysis reaction. This seems to be always the case if a mixture of protic and aprotic solvents is encapsulated in RMs of AOT. Hence, the aprotic solvent—in which the substrate is usually more soluble, even if it is not favorable for the enzyme activity—upon encapsulation is excluded from the reaction site, and an important overall increase in the reaction rate is observed. At present, we also have preliminary results that show that ionic liquids that inhibit completely the enzyme performance in homogeneous media, are surprisingly good upon encapsulation with water in RMs.

Altogether, our results highlight the importance of RMs as nanoreactor media for enzymatic reactions, in which the enzyme not only retains but increases its activity in comparison with homogeneous media, even in the presence of solvents such as DMF or DMSO, which act as inhibitors. We hope to stimulate the scientific community to use these fascinating and unique nanoreactors to perform different types of chemical reactions, including with enzymes other than  $\alpha$ -CT and for nanoparticle synthesis.

## Experimental Section

### General

AOT (>99% purity, Sigma–Aldrich) was used as received and was kept under vacuum over P<sub>2</sub>O<sub>5</sub> to minimize water absorption. The absence of acidic impurities was confirmed using the solvatochromism of 1-methyl-8-oxoquinolinium betaine.<sup>[43]</sup>

$\alpha$ -CT (molecular weight 24800, from bovine pancreas), and 2-NA (Sigma–Aldrich) were purchased from Sigma–Aldrich and used as received. *n*-heptane (Sintorgan HPLC), GY and DMF (both fluorescence spectroscopy quality, from Merck) were used without purification. Ultrapure water was used throughout and prepared to a specific resistivity of >18 M $\Omega$  cm (Labonco equipment model 90901-01). The solvent mixtures used were GY/DMF/water (20:20:60, v/v/v), DMF/water (20:80, v/v) and GY/water (40:60, v/v).

The pH of the bulk solutions (water or mixtures) was maintained at 8.7 by using phosphate buffer (20 mM). The pH cannot be measured inside the polar core of the RM aggregate.<sup>[43]</sup> A meaningful approximation to the pH within the aqueous pseudophase of the RMs can be made using pure AOT with sufficient buffering capacity

in the bulk solutions (i.e., such that the observed rates are independent of the buffer concentrations).<sup>[44]</sup> In this sense, the value of the pH inside the polar core is referenced to the homogeneous buffer solution, and is termed  $\text{pH}_{\text{ext}}$ . Nevertheless, as the concept of pH inside RMs is a matter of discussion,<sup>[43,45]</sup> we measured the kinetics with no buffer solution and the results were the same, that is, the kinetic parameters do not depend on the presence of buffer.

DLS experiments were performed at a fixed surfactant concentration of 0.1 M and therefore the RM solutions are not at infinite dilution. Thus, it is appropriate to introduce an apparent hydrodynamic diameter ( $d_{\text{app}}$ ), in order to make the comparison with the system studied here. A similar approach has been used previously.<sup>[46]</sup> The  $d_{\text{app}}$  values of the different RM systems were determined by DLS on a Malvern 4700 instrument with a goniometer and an argon ion laser operating at  $\lambda = 488$  nm. Cleanliness of the cuvettes used for measurements was of crucial importance for obtaining reliable and reproducible data.<sup>[47]</sup> Cuvettes were washed with ethanol, and then with doubly distilled water, and dried with acetone. Prior to use, the samples were filtered three times to avoid dust or particles present in the original solution, using an Acrodisc syringe filter with a 0.2  $\mu\text{m}$  PTFE membrane (Sigma-Aldrich) for the RM samples. Prior to data acquisition, the samples were allowed to equilibrate in the DLS instrument for 10 min at 25 °C. To obtain valid results from DLS measurements, knowledge of the system's refractive index and viscosity, in addition to well-defined conditions is required. The refractive indices and viscosities for the AOT RMs were assumed to be the same as neat *n*-heptane. Multiple samples at each size were made, and 30 independent size measurements were performed for each individual sample at the scattering angle of 90°. The instrument was calibrated before and during the course of experiments, using several different size standards. Thus, the magnitudes obtained by DLS measurements can be taken as statistically meaningful for all the systems investigated. The algorithm used was CONTIN and the DLS experiments showed that the polydispersity of the AOT RMs was less than 5%.

## Methods

Mixed solvents were prepared by mixing the required volume of solvent to obtain the required % v/v. A stock solution of 2-NA (0.01 M) in the different solvent mixtures and in pure water was also prepared.

For kinetic measurements in homogeneous media, solutions of  $\alpha$ -CT (3 mL) in various mixed solvents and water [phosphate buffer (20 mM), pH 8.7,  $[\alpha\text{-CT}] = 5 \times 10^{-6}$  M] at the required molar ratio were introduced into a thermostated cell. Then, the enzymatic reaction was initiated by addition of different  $\mu\text{L}$  quantities of stock solutions of 2-NA in order to have a total volume of 3 mL of solution at the desired 2-NA concentration. For example, for  $[2\text{-NA}] = 1 \times 10^{-3}$  M, 30  $\mu\text{L}$  of stock solution was added to the cell. The concentration of 2-NA was varied between  $10^{-3}$  and  $10^{-2}$  M.

## Calculation of the 2-NA Partition Constant in Homogeneous Media

The partition constant values in homogeneous media,  $K_{\text{p}}^{\text{mixture}/n\text{-heptane}}$ , for the 2-NA distribution between DMF/water or GY/DMF/water mixture and *n*-heptane were determined by the hand-shaking method.<sup>[48]</sup> Solutions of 2-NA were prepared in different solvent mixtures and the absorbance at  $\lambda_{\text{abs}} = 314$  nm, the maximum absorbance wavelength of 2-NA in *n*-heptane, was mea-

sured. Afterwards, this mixture (5 mL) was added to *n*-heptane (5 mL). After shaking the mixture for about 5 min, the *n*-heptane phase was extracted and its absorbance measured. The  $K_{\text{p}}^{\text{mixture}/n\text{-heptane}}$  was determined according to Equation (4):

$$K_{\text{p}}^{\text{mixture}/n\text{-heptane}} = [(A_0 - A)/A] V_{\text{org}}^{-1} V_{\text{mixture}} \quad (4)$$

where  $A_0$  is the absorbance of the 2-NA in *n*-heptane before the extraction with the mixture,  $A$  is the absorbance in the same phase after extraction with the mixture,  $V_{\text{mixture}}$  is the volume of the phase mixture and  $V_{\text{org}}$  is the volume of the organic phase.

## Reaction in Mixed Solvent/AOT/*n*-Heptane RMs

A stock solution of AOT in *n*-heptane was prepared by weighing 17.28 g of the surfactant dissolved in 100 mL to reach a concentration of 0.4 M. Stock solutions of  $\alpha$ -CT in phosphate buffer (20 mM) and 2-NA ( $1 \times 10^{-2}$  M) in different mixed solvents and in pure water were prepared. The values of  $W_{\text{GY/water}}$  and  $W_{\text{DMF/water}}$  in the mixtures of polar solvents have two contributions [see Eqs. (5) and (6)] and  $W_{\text{T}}$  has three contributions [Eq. (7)].

$$W_{\text{GY/water}} = ([\text{GY}] + [\text{water}])/[\text{AOT}] = W_{\text{GY}} + W_{\text{water}} \quad (5)$$

$$W_{\text{DMF/water}} = ([\text{DMF}] + [\text{water}])/[\text{AOT}] = W_{\text{DMF}} + W_{\text{water}} \quad (6)$$

$$W_{\text{T}} = ([\text{GY}] + [\text{DMF}] + [\text{water}])/[\text{AOT}] = W_{\text{GY}} + W_{\text{DMF}} + W_{\text{water}} \quad (7)$$

where  $W_{\text{GY}}$ ,  $W_{\text{DMF}}$  and  $W_{\text{water}}$  represent the values of the molar ratio between each of the polar solvents and the AOT, respectively. In the RM media, the water, GY/water, DMF/water and GY/DMF/water molar ratios were expressed in terms of  $W_{\text{GY}}$ ,  $W_{\text{DMF}}$  and  $W_{\text{water}}$  which are equivalent to the molar ratio composition in homogeneous media.

A stoppered cell was filled with AOT solution (3 mL) at the appropriate concentration. The desired  $W_{\text{water}}$  value was achieved by adding sufficient stock  $\alpha$ -CT phosphate buffer solution with a microsyringe in order to obtain  $[\alpha\text{-CT}] = 5 \times 10^{-6}$  M, and the mixture was shaken until a clear solution was obtained. Once the desired  $W_{\text{GY}}$  and  $W_{\text{DMF}}$  values were reached, the enzymatic reaction was initiated by adding the appropriate volume of the stock 2-NA solution in water to give the desired  $W_0$  values.

## Calculation of the 2-NA Partition Constant in RM Media

The partitioning of 2-NA between the RMs and the organic solvent pseudophases can be considered within the framework of the pseudophase model.<sup>[4,14,49-51]</sup> This model considers the RMs to be distinct pseudophases, the properties of which are independent of the AOT concentration and are only determined by the value of the characteristic parameter  $W$ . In this model, only two solubilization sites are considered, that is, the external nonpolar solvent and the RMs (i.e., all the surfactant molecules). Hence, the distribution of 2-NA between the micelles and the external solvent pseudophase defined in Equation (8) can be expressed in terms of the partition constant  $K_{\text{p}}$  [Eq. (9)]:

$$[2\text{-NA}]_{\text{f}} \rightleftharpoons [2\text{-NA}]_{\text{b}} \quad (8)$$

$$K_{\text{p}} = \frac{[2\text{-NA}]_{\text{b}}^{\#}}{[2\text{-NA}]_{\text{f}}} \quad (9)$$

The terms in brackets represent the local concentrations of free (f) and bound (b) 2-NA, that is, the concentration expressed in terms of the volume of the RMs.<sup>[4]</sup> If  $[2\text{-NA}]_b$  is the analytical concentration of micelle-bound substrate, Equation (10) holds:

$$[2\text{-NA}]_b^{\#} = \frac{[2\text{-NA}]_b}{[\text{AOT}]} \quad (10)$$

and  $K_p$  can be expressed as in Equation (11):

$$K_p = \frac{[2\text{-NA}]_b}{[2\text{-NA}]_f [\text{AOT}]} \quad (11)$$

where  $[2\text{-NA}]_f$  is the concentration of the substrate in *n*-heptane, and  $[\text{AOT}]$  is surfactant concentration. This equation applies at a fixed value of  $W$  and if  $[2\text{-NA}]_T \ll [\text{AOT}]$ , where  $[2\text{-NA}]_T$  is the probe analytical concentration.

## Acknowledgements

Financial support from the Consejo Nacional de Investigaciones Científicas y Técnicas (CONICET), Universidad Nacional de Río Cuarto, Agencia Nacional de Promoción Científica y Técnica and Agencia Córdoba Ciencia is gratefully acknowledged. R.D.F., N.M.C., J.J.S. hold research positions at CONICET. A.M.D. thanks CONICET for a research fellowship during his Ph.D.

**Keywords:** aggregates · enzyme catalysis · reverse micelles · self-assembly · solvent mixtures

- [1] D. M. Davis, D. McLoskey, D. J. Birch, P. R. Gellert, R. S. Kittlety, R. M. Swart, *Biophys. Chem.* **1996**, *60*, 63–77.
- [2] T. K. De, A. Maitra, *Adv. Colloid Interface Sci.* **1995**, *59*, 95–193.
- [3] S. P. Moulik, B. K. Paul, *Adv. Colloid Interface Sci.* **1998**, *78*, 99–195.
- [4] J. J. Silber, A. Biasutti, E. Abuin, E. Lissi, *Adv. Colloid Interface Sci.* **1999**, *82*, 189–252.
- [5] P. Hazra, D. Chakrabarty, N. Sarkar, *Langmuir* **2002**, *18*, 7872–7879.
- [6] H. B. Bohidar, M. Behboudnia, *Eur. Polym. J.* **2000**, *36*, 2463–2470.
- [7] H. Bohidar, M. Behboudnia, *Colloids Surf. A* **2001**, *178*, 313–323.
- [8] N. M. Correa, J. J. Silber, R. E. Riter, N. E. Levinger, *Chem. Rev.* **2012**, *112*, 4569–4602.
- [9] A. M. Durantini, R. D. Falcone, J. J. Silber, N. M. Correa, *ChemPhysChem* **2009**, *10*, 2034–2040.
- [10] A. M. Durantini, R. D. Falcone, J. J. Silber, N. M. Correa, *J. Phys. Chem. B* **2013**, *117*, 3818–3828.
- [11] A. M. Durantini, R. D. Falcone, J. J. Silber, N. M. Correa, *J. Phys. Chem. B* **2011**, *115*, 5894–5902.
- [12] R. D. Falcone, J. J. Silber, N. M. Correa, *Phys. Chem. Chem. Phys.* **2009**, *11*, 11096–11100.
- [13] K. Martinek, I. V. Berezin, Y. L. Khmel'nitski, N. L. Klyachko, A. V. Levashov, *Collect. Czech. Chem. Commun.* **1987**, *52*, 2589–2602.
- [14] M. A. Biasutti, E. B. Abuin, J. J. Silber, N. M. Correa, E. A. Lissi, *Adv. Colloid Interface Sci.* **2008**, *136*, 1–24.
- [15] F. Mayer, M. Hoppert, *Naturwissenschaften* **1996**, *83*, 36–39.
- [16] M. Hirai, T. Takizawa, S. Yabuki, R. Kawai-Hirai, M. Oya, K. Nakamura, K. Kobashi, Y. Amemiya, *J. Chem. Soc. Faraday Trans.* **1995**, *91*, 1081–1089.
- [17] E. Ruckenstein, P. Karpe, *J. Colloid Interface Sci.* **1990**, *139*, 408–436.
- [18] F. Moyano, R. D. Falcone, J. C. Mejuto, J. J. Silber, N. M. Correa, *Chem. Eur. J.* **2010**, *16*, 8887–8893.
- [19] N. W. Fadnavis, R. L. Babu, A. Deshpande, *Biochimie* **1998**, *80*, 1025–1030.
- [20] R. D. Falcone, M. A. Biasutti, N. M. Correa, J. J. Silber, E. Lissi, E. Abuin, *Langmuir* **2004**, *20*, 5732–5737.
- [21] A. Kumar, P. Venkatesu, *Chem. Rev.* **2012**, *112*, 4283–4307.
- [22] F. Zaera, *Chem. Soc. Rev.* **2013**, *42*, 2746–2762.
- [23] T. E. Sintra, S. P. M. Ventura, J. A. P. Coutinho, *J. Mol. Catal. B* **2014**, *107*, 140–151.
- [24] N. V. Nucci, K. G. Valentine, A. J. Wand, *J. Magn. Reson.* **2014**, *241*, 137–147.
- [25] R. W. Peterson, M. S. Pometun, Z. Shi, A. J. Wand, *Protein Sci.* **2005**, *14*, 2919–2921.
- [26] F. Moyano, E. Setien, J. J. Silber, N. M. Correa, *Langmuir* **2013**, *29*, 8245–8254.
- [27] J. F. Bello, E. F. Llama, C. del Campo, M. J. Cabezas, J. V. Sinisterra, M. S. Arias, *J. Mol. Catal.* **1993**, *78*, 91–112.
- [28] T. Kijima, S. Yamamoto, H. Kise, *Enzyme Microb. Technol.* **1996**, *18*, 2–6.
- [29] R. Sengwa, V. Khatri, S. Sankhla, *Fluid Phase Equilib.* **2008**, *266*, 54–58.
- [30] L. Xu, X. Hu, R. Lin, *J. Solution Chem.* **2003**, *32*, 363–370.
- [31] B. Paiecz, H. Piekarski, *J. Solution Chem.* **1997**, *26*, 621–629.
- [32] G. DiPaola, B. Belleau, *Can. J. Chem.* **1977**, *55*, 3825–3830.
- [33] L. Yu, Y. Zhu, X.-G. Hu, X.-H. Pang, *J. Chem. Eng. Data* **2006**, *51*, 1110–1114.
- [34] E. Abuin, E. Lissi, R. Bridi, *J. Chil. Chem. Soc.* **2011**, *56*, 948–950.
- [35] Y. L. Khmel'nitskiy, A. Kabanov, N. Klyachko, A. Levashov, K. Martinek in *Enzymatic Catalysis in Reverse Micelles*, Elsevier Scientific, Amsterdam, **1989**, pp. 230–261.
- [36] P. D. I. Fletcher, M. F. Galal, B. H. Robinson, *J. Chem. Soc. Faraday Trans. 1* **1984**, *80*, 3307–3314.
- [37] R. E. Riter, J. R. Kimmel, E. P. Undiks, N. E. Levinger, *J. Phys. Chem. B* **1997**, *101*, 8292–8297.
- [38] Y. Miyake, T. Owari, F. Ishiga, M. Teramoto, *J. Chem. Soc. Faraday Trans.* **1994**, *90*, 979–986.
- [39] E. Lissi, D. Engel, *Langmuir* **1992**, *8*, 452–455.
- [40] L. F. Aguilar, E. Abuin, E. Lissi, *Arch. Biochem. Biophys.* **2001**, *388*, 231–236.
- [41] E. A. Lissi, E. B. Abuin, *Langmuir* **2000**, *16*, 10084–10086.
- [42] N. M. Correa, M. A. Biasutti, J. J. Silber, *J. Colloid Interface Sci.* **1995**, *172*, 71–76.
- [43] B. Baruah, J. M. Roden, M. Sedgwick, N. M. Correa, D. C. Crans, N. E. Levinger, *J. Am. Chem. Soc.* **2006**, *128*, 12758–12765.
- [44] P. D. Fletcher, R. B. Freedman, J. Mead, C. Oldfield, B. H. Robinson, *Colloids Surf.* **1984**, *10*, 193–203.
- [45] O. F. Silva, M. A. Fernández, J. J. Silber, R. H. de Rossi, N. M. Correa, *ChemPhysChem* **2012**, *13*, 124–130.
- [46] A. Salabat, J. Eastoe, K. J. Mutch, R. F. Tabor, *J. Colloid Interface Sci.* **2008**, *318*, 244–251.
- [47] M. A. Sedgwick, A. M. Trujillo, N. Hendricks, N. E. Levinger, D. C. Crans, *Langmuir* **2011**, *27*, 948–954.
- [48] E. Abuin, E. Lissi, M. A. Biasutti, R. Duarte, *Protein J.* **2007**, *26*, 475–479.
- [49] E. Abuin, E. Lissi, R. Duarte, J. Silber, M. Biasutti, *Langmuir* **2002**, *18*, 8340–8344.
- [50] M. Encinas, E. Lissi, *Chem. Phys. Lett.* **1986**, *132*, 545–548.
- [51] P. N. Hurter, P. Alexandridis, T. Hatton in *Solubilization in Surfactant Aggregates* (Eds.: S. D. Christian, J. F. Scamehorn), Marcel Dekker, New York, **1995**, pp. 191–235.

Manuscript received: December 22, 2015

Revised: February 10, 2016

Accepted Article published: February 19, 2016

Final Article published: March 16, 2016